PHYSICAL REVIEW B **96**, 064410 (2017)

Temperature dependence of spin-orbit torques across the magnetic compensation point in a ferrimagnetic TbCo alloy film

Kohei Ueda,* Maxwell Mann, Paul W. P. de Brouwer, David Bono, and Geoffrey S. D. Beach†
Department of Materials Science and Engineering, Massachusetts Institute of Technology, Cambridge, Massachusetts 02139, USA
(Received 7 March 2017; revised manuscript received 25 June 2017; published 7 August 2017)

The temperature dependence of spin-orbit torques (SOTs) and spin-dependent transport parameters is measured in bilayer Ta/TbCo ferrimagnetic alloy films with bulk perpendicular magnetic anisotropy. We find that the dampinglike (DL)-SOT effective field diverges as temperature is swept through the magnetic compensation temperature (T_M), where the net magnetization vanishes due to the opposing contributions from the Tb and Co sublattices. We show that DL-SOT scales with the inverse of the saturation magnetization (M_s), whereas the spin-torque efficiency is independent of the temperature-dependent M_s. Our findings provide insight into spin transport mechanisms in ferrimagnets and highlight low-M_s rare-earth/transition-metal alloys as promising candidates for SOT device applications.

DOI: 10.1103/PhysRevB.96.064410

In the last five years, ferromagnetic films in contact with heavy metals with strong spin-orbit coupling have attracted interest for their potential utility in nonvolatile random access memory elements. In these systems, current-induced spin-orbit torques (SOTs) [1,2] on the magnetization can be induced by the Rashba-Edelstein effect at the interface [3,4] and by spin currents injected from the heavy metal due to the spin Hall effect [2,5–26]. SOTs with both a fieldlike and dampinglike character can manifest in such systems, with the latter capable of driving magnetization switching [1–5,7,9,11–13,15,21,22,24] and magnetic domain wall motion [26–31]. SOTs have been identified and quantified by a variety of techniques including spin-torque ferromagnetic resonance [2,7,14,17,19,25], quasistatic magnetization tilting probed through harmonic voltage measurements [6,8–13,17,19–26,28,31], and current-induced hysteresis loop shift measurements [18,32,33]. Most studies of SOTs have focused on ultrathin metallic ferromagnet/heavy-metal bilayers with interfacial perpendicular magnetic anisotropy (PMA) [1–3,5–9,11–13,15–26].

Unlike ferromagnetic systems with interfacial PMA, ferrimagnetic films based on rare-earth (RE)–transition-metal (TM) alloys possess strong bulk PMA [31–44] as well as a low net magnetization. Moreover, the net magnetization can be tuned by the composition and temperature [32,34–36,38], making these materials of great interest for examining phenomena such as ultrafast optical switching [35–38], current-induced switching [39], and domain wall motion [31,40–42], which rely on maximizing the torque exerted on the net magnetization. Since these materials consist of two magnetic sublattices whose magnetic moments possess different orbital character, their dynamics and interactions with spin currents are especially rich. Recently, SOTs in ferrimagnet/heavy-metal bilayer films have been investigated, and the transport mechanisms were discussed [31–33,43,44]. Finley and Liu reported a maximum in the dampinglike SOT efficiency at the smallest net magnetization in Ta/Tb_xCo_{1-x} bilayer films grown with a series of different compositions [32] measured at room temperature. However, a systematic temperature-dependent study of spin-transport and SOTs near the magnetization compensation temperature is lacking. For example, it is known that the anomalous Hall effect (AHE) in RE-TM alloys tracks the TM sublattice magnetization [32,33,44,45], implying predominant spin-dependent interactions with the 3*d* orbitals as opposed to the magnetic 4*f* orbitals on the RE atoms. If the dampinglike SOT likewise interacts predominantly with one sublattice, then the current-induced effective field should vary smoothly through the compensation temperature, whereas if it is exerted on the net magnetization, then the effective field should diverge. A temperature-dependent study can hence provide insight into the mechanisms of spin absorption in multisublattice systems in a single sample, in which structure, composition, and interface characteristics are fixed, and only the relative sublattice moments are tuned.

In this paper, to further understand the relation between magnetic properties and spin-transport mechanisms, we investigate the temperature dependence of SOTs, spin-dependent transport, and magnetic properties in a bilayer Ta/TbCo film as temperature is swept through the magnetization compensation temperature T_M. We show that the effective field from the dampinglike SOT diverges near T_M, whereas the spin-torque efficiency is relatively constant with temperature. However, the coercive field also diverges near T_M, so that the switching efficiency is not expected to be enhanced. We also find that the magnitude of the AHE is relatively constant with temperature but its sign inverts at T_M, while the planar Hall effect (PHE) increases with decreasing temperature.

We fabricated the layer structure substrate/Ta(8)/$Tb_{19}Co_{81}$(6.5)/TaOx(3) by dc magnetron sputtering, where the numbers in parentheses indicate the layer thicknesses in nm. The alloy $Tb_{19}Co_{81}$ was grown by cosputtering, and the composition was estimated from the relative deposition rates of Tb and Co. TbCo films at this composition are known to exhibit an amorphous structure [32,34,38]. According to previous studies [32–34,38], the magnetization of this film is expected to be Co-dominated at room temperature. The film was grown on a Ta underlayer that acts as a buffer layer and a SOT source due to the spin Hall effect [2,6,8,18,32,33]. The film was

*kubond@mit.edu
†gbeach@mit.edu

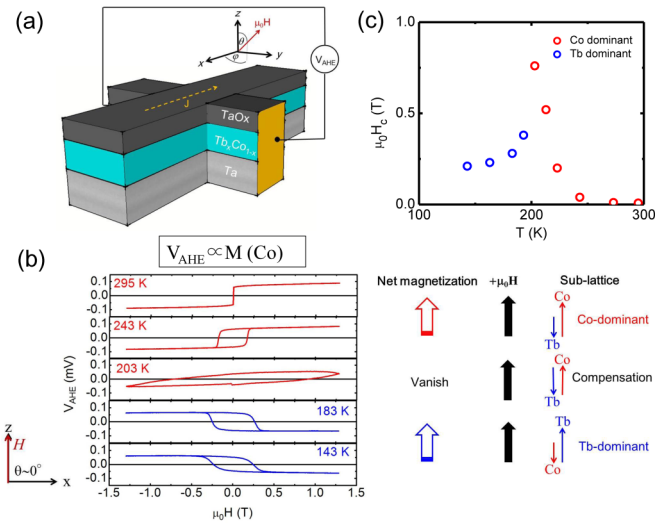

FIG. 1. (a) Schematic illustration of a device with Hall cross structure and measurement setup. Current is applied along the x axis and anomalous Hall effect voltage is measured along the y axis. (b) AHE hysteresis loops under external magnetic field $\mu_0 H$ at polar angle, $\theta = 0^\circ$ for various temperatures. Left sketch shows the orientation of $\mu_0 H$. Right sketch denotes schematically the direction of the sublattice magnetizations under $\mu_0 H$ in Co or Tb dominated films. Total net magnetization vanishes when the magnetization on the two sublattices are equal in magnitude, defining the magnetic compensation temperature T_M. (c) Coercive field $\mu_0 H_c$ as a function of temperature. Upon crossing T_M, the sublattice dominating the net magnetization transitions between Co (red symbols) and Tb (blue symbols).

capped with a naturally oxidized TaOx layer to protect the TbCo film. For transport measurements, a device with a Hall cross structure, with channel dimension 10 μm long by 5 μm wide, was patterned by photolithography and postdeposition lift-off. Ta(3)/Au(54) contact pads were then patterned at the ends of the device for electrical measurements. Figure 1(a) shows schematically the device structure and the measurement configuration. Current was applied along the x axis and the AHE voltage V_{AHE} was measured along the y direction. θ and φ represent the polar and azimuthal angles, respectively, of the applied magnetic field $\mu_0 H$. Temperature-dependent measurements were conducted in a gas-flow cryostat.

We first examined the temperature dependence of the magnetic properties. A series of out-of-plane hysteresis loops at several temperatures is shown in Fig. 1(b), measured via the AHE voltage using a standard lock-in technique. The loops all exhibit an out-of-plane easy axis consistent with PMA. With decreasing temperature, the coercivity $\mu_0 H_c$ is found to increase and then decrease [Fig. 1(c)], at which point the sign of the AHE voltage V_{AHE} reverses. This behavior is explained schematically in Fig. 1(b). Close to T_M, the total net magnetization approaches zero since the magnetizations of two sublattices are equal in magnitude. At this temperature, the coercivity diverges since the torque from the applied field scales inversely with saturation magnetization M_s. The reversal of the sign of V_{AHE} is in good agreement with previous studies reporting that the AHE originates predominantly from spin-dependent interactions with the TM sublattice [32,33,44,45].

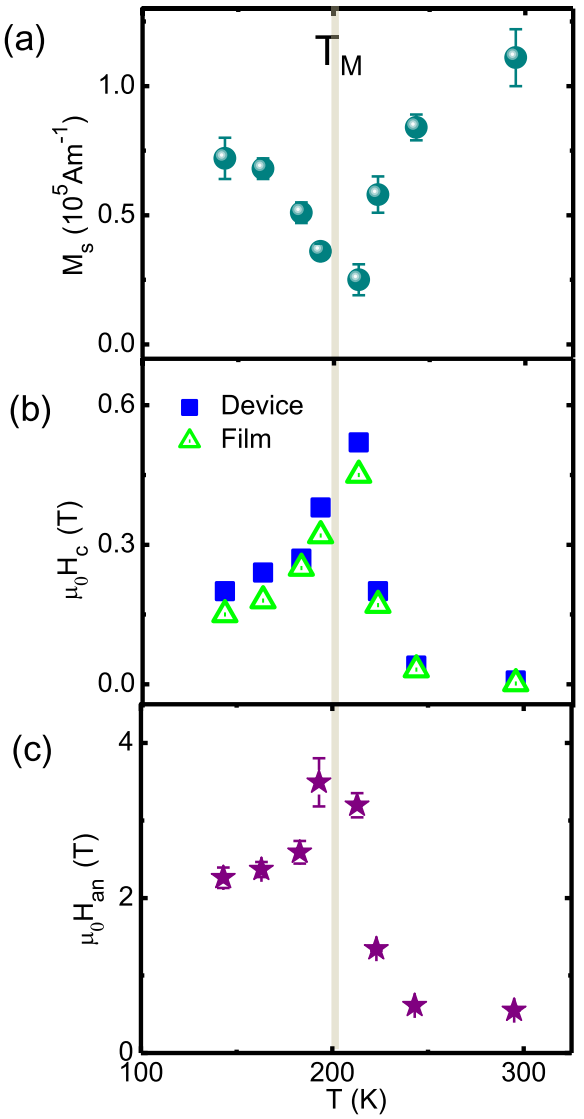

FIG. 2. Temperature dependence of (a) saturation magnetization, (b) coercivity $\mu_0 H_c$ of patterned device and continuous film, and (c) magnetic anisotropy field $\mu_0 H_{an}$. Magnetization compensation temperature is marked by T_M.

From these data we estimate $T_M \sim 200$ K, below (above) which the Tb (Co) sublattice dominates M_s.

Figure 2(a) shows M_s versus temperature, measured with a vibrating sample magnetometer (VSM) on a companion film grown simultaneously with the patterned device. The coercivity measured by VSM corresponds closely with that measured by the AHE on the patterned device, as seen in Fig. 2(b). Finally, the perpendicular anisotropy field $\mu_0 H_{an}$ [Fig. 2(c)] was obtained by fitting the curvature of the AHE voltage signal versus in-plane field to the Stoner-Wolfarth model to describe uniform tilting of the magnetization away from the easy axis. As can be seen, the minimum in M_s and the maximum in $\mu_0 H_c$ and $\mu_0 H_{an}$ all coincide.

We next examine SOTs and their variation with temperature through T_M. In order to quantify the SOT effective fields, we performed conventional harmonic voltage measurements using a lock-in amplifier [6,8,12]. An applied ac current

causes SOTs that produce a small periodic oscillation of the magnetization about its equilibrium orientation. This generates first-harmonic ($V_{\omega 1}$) and second-harmonic ($V_{\omega 2}$) Hall voltage signals whose in-plane field dependence can be used to quantify the effective fields corresponding to the dampinglike (H_{DL}) and fieldlike (H_{FL}) SOTs.

For all temperatures, $\mu_0 H$ was swept quasistatically between ± 1.3 T, while $V_{\omega 1}$ and $V_{\omega 2}$ were measured using an ac current with amplitude 1.1 mA and angular frequency $\omega = 3.5$ kHz. $\mu_0 H$ was applied parallel to the current direction ($\varphi = 0^\circ$) to measure H_{DL} and perpendicular to current ($\varphi = 90^\circ$) to measure H_{FL}. To avoid a multidomain state, the field was oriented at $\theta = 72^\circ$ so as to include a finite out-of-plane component. We repeated the measurements for several polar angles to verify that the results below are independent of θ except for small (or zero) θ, at which we observe a decreased V_{AHE} signal indicative of a multidomain state when the in-plane field component is large.

Figure 3(a) shows typical $V_{\omega 1}$ loops at 243 and 183 K, with field applied at $\theta = 72^\circ$ and $\varphi = 0^\circ$. Figures 3(b) and 3(c) show $V_{\omega 2}$ measured at these same temperatures with the field along $\varphi = 0^\circ$ and $\varphi = 90^\circ$, respectively, both with $\theta = 72^\circ$. We find that the signs of the $V_{\omega 1}$ and $V_{\omega 2}$ loops invert across T_{M} as expected since the sign of the AHE voltage reverses [44].

Quite recently, Yu *et al.* has shown two ways for fitting $V_{\omega 2}$, in the low-field and high-field regimes (with respect to the anisotropy field): below $\mu_0 H_{\mathrm{an}}$ a linear fit is performed, whereas above $\mu_0 H_{\mathrm{an}}$ a parabolic fit is performed, as the magnetization tilts toward the film plane [24]. Due to the limited range of our electromagnet, the high-field regime cannot be reached for all temperatures, so we have analyzed the data in the low-field regime where $V_{\omega 2}$ is linear, using the following relations [6,13,44]:

$$H'_{\mathrm{DL(FL)}} = -2\left(\frac{\partial V_{\omega 2}}{\partial H_{x(y)}}\right) \times \left(\frac{\partial^2 V_{\omega 1}}{\partial H_{x(y)}^2}\right)^{-1}, \tag{1}$$

$$H_{\mathrm{DL(FL)}} = \frac{H'_{\mathrm{DL(FL)}} \pm 2\zeta H'_{\mathrm{FL(DL)}}}{1 - 4\zeta^2}. \tag{2}$$

Here, H_x, H_y indicate the field components along the x- and y axes, respectively, and in Eq. (2), positive and negative signs correspond to the cases with the z component of the magnetization along $+z$ and $-z$ respectively. Finally, ζ is the ratio of PHE and AHE coefficients $\zeta = {}^{R_{\mathrm{PHE}}}/_{R_{\mathrm{AHE}}}$; the former was obtained by measuring the Hall voltage with the field oriented at $\varphi = 45^\circ$ as described in Refs. [8,12,13,24]. Additionally, the anomalous Nernst effect (ANE) may give an additional contribution to $V_{\omega 2}$ due to current-induced inhomogeneous heating [8]. We found that our sample exhibited negligible ANE contribution by measuring $V_{\omega 2}$ at $\theta = 0$ [8,12].

Figure 4 summarizes the temperature dependence of the spin-transport parameters and SOT effective fields. We find that the sign of R_{AHE} reverses across T_{M}, whereas its magnitude varies only weakly with temperature [Fig. 4(a)], which suggests that it follows the Co sublattice magnetization, which does not change much with temperature within this range. Similarly, R_{PHE}, reverses sign across T_{M} but its magnitude does not vary considerably in this temperature range, which is reasonable since the AHE and PHE are geometrically related [45,46].

The temperature dependence of the dampinglike and fieldlike effective fields per unit current density, defined as $\chi_{\mathrm{DL(FL)}} = \mu_0 H_{\mathrm{DL(FL)}}/J$, are shown in Figs. 4(c) and 4(d), respectively. In computing $\chi_{\mathrm{DL(FL)}}$, we estimated the current flowing in the bottom Ta layer assuming a parallel resistor model, based on the experimentally obtained resistivity of TbCo (290 $\mu\Omega$cm) and Ta (370 $\mu\Omega$cm) thin films. The fraction of current flowing through the Ta layer is estimated to be 51% for 6.5-nm-thick TbCo and 49% for 8-nm-thick Ta, respectively. Measurements of the device resistance and separate measurements of the sheet resistance of a thin Ta film both show a resistance change of only <2% of the measurement range, so in our calculations we assumed that the current distribution between the two layers is constant with temperature. In Fig. 4 it is seen that χ_{DL} varies strongly with temperature and diverges near T_{M} where the net magnetization vanishes, consistent with previous work reported by Finley and Liu [32]. By contrast, χ_{FL} is relatively independent of temperature (and hence M_s), and is about an order of magnitude smaller than χ_{DL}.

Finally, the dampinglike spin-torque efficiency ξ_{DL} was calculated according to $H_{\mathrm{DL}}/J = \hbar\xi_{\mathrm{DL}}/(2eM_s t_{\mathrm{TbCo}})$ [17], where e is the electron charge, $\hbar$ is the reduced Planck constant, and t_{TbCo} is the thickness of TbCo. Assuming

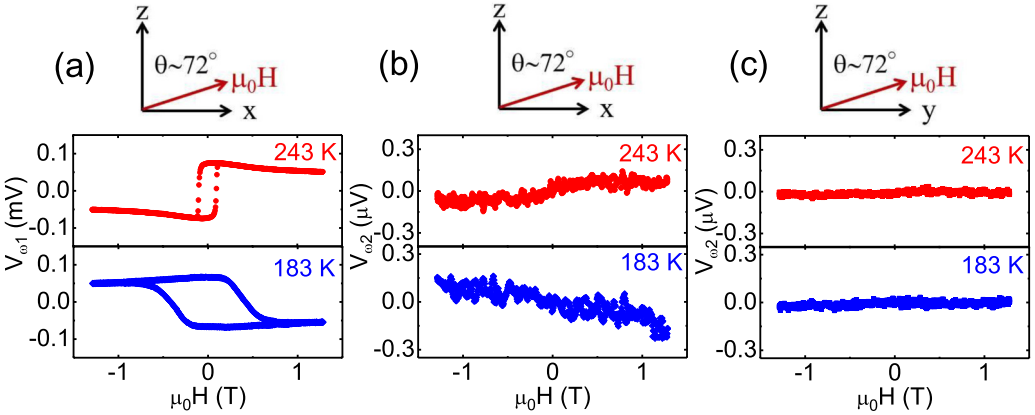

FIG. 3. (a) First- and (b) second-harmonic voltage response loops with $\mu_0 H$ at $\theta = 72^\circ$ and $\varphi = 0^\circ$. (c) Second-harmonic voltage measurements at $\theta = 72^\circ$ and $\varphi = 90^\circ$. Sketches indicate orientation of the applied field.

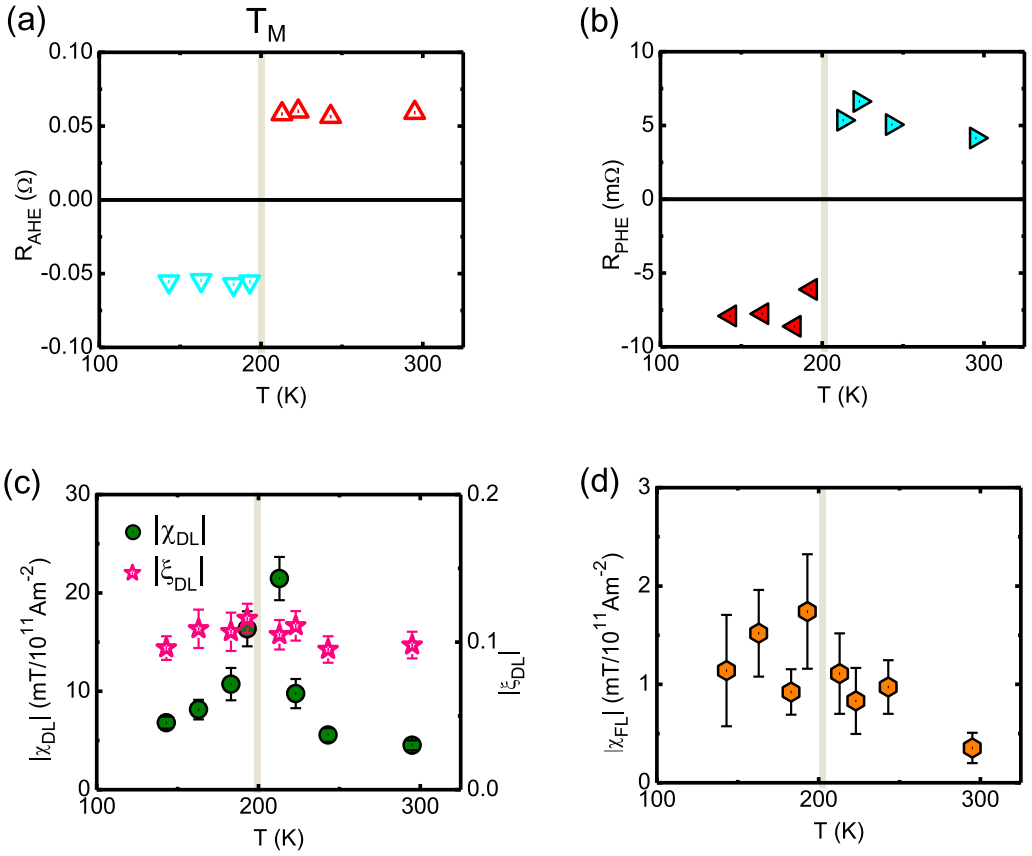

FIG. 4. Temperature dependence of (a) anomalous Hall coefficient R_{AHE}, (b) planar Hall coefficient R_{PHE}, (c) dampinglike effective field per unit current density χ_{DL} and spin-torque efficiency ξ_{DL}, and (d) effective field per unit current density χ_{FL} from fieldlike torque. Gray vertical line indicates magnetic compensation temperature T_{M}.

the dampinglike SOT derives predominantly from the spin Hall effect (i.e., neglecting contributions from an interfacial Rashba-like interaction) in the Ta layer, ξ_{DL} is related to the internal spin Hall angle θ_{SH} of Ta and the interfacial spin transparency T_{int} through $\xi_{\mathrm{DL}} = \theta_{\mathrm{SH}} T_{\mathrm{int}}$. The coefficient of spin transparency in a normal metal/magnetic metal bilayer can be written $T_{\mathrm{int}} = 2G_{\mathrm{eff}}^{\uparrow\downarrow}/G_{\mathrm{NM}}$, where $G_{\mathrm{eff}}^{\uparrow\downarrow}$ is the interfacial spin-mixing conductance and G_{NM} is the spin conductance of the normal metal [17]. We find $\xi_{\mathrm{DL}} < 0$ at all temperatures, consistent with the negative spin Hall angle of Ta [2], and that $|\xi_{\mathrm{DL}}| \approx 0.1$, independent of temperature. Since the spin Hall angle of Ta has been reported to vary by less than 10% within this temperature range [15], this result suggests that the spin-mixing conductance is independent of temperature despite the strong variation of M_{s} with temperature.

The above discussion indicates that spin transport and SOTs show critical behaviors near the magnetization compensation temperature T_{M}. There is also an angular momentum compensation temperature T_{A}, where the angular momentum is zero although the net magnetization is nonzero, due to the different g factors of RE and TM atoms. One might expect that since the Slonczewski-like torque is framed in terms of transfer of angular momentum, its divergence should occur near T_{A} rather than T_{M}. Hence, our results for the SOT effective field are particularly surprising and unexpected. Previously, Stanciu *et al.* [35] and Binder *et al.* [36] have demonstrated ultrafast switching as well as a divergence of the damping constant near T_{A} (not T_{M}) using optical pump probe and vector network analyzer-ferromagnetic resonance techniques. While at T_{M} one has $M_{\mathrm{TM}} = M_{\mathrm{RE}}$, at T_{A} one has $\frac{M_{\mathrm{TM}}}{\gamma_{\mathrm{TM}}} = \frac{M_{\mathrm{RE}}}{\gamma_{\mathrm{RE}}}$ with $\gamma_{\mathrm{TM(RE)}} = -\frac{g\mu_B}{\hbar}$, where $\gamma_{\mathrm{TM(RE)}}$ is the gyromagnetic ratio, μ_{B} is the Bohr magneton, and g is the Landé g factor that accounts for the relative contribution of orbital and spin angular momentum to the total angular momentum. Based on the expression above, our TbCo composition is expected to have $T_{\mathrm{M}} < T_{\mathrm{A}}$ considering the g factors of Co (∼2.2) and Tb (∼1.5) [47,48] and the weak temperature dependence of the Co sublattice magnetization in the measurement range. The difference between T_{M} and T_{A} is ∼50 K for GdFeCo [35] and ∼80 K for GdCo [36], and our TbCo is expected to show a greater temperature difference, with $T_{\mathrm{A}} > 300$ K. Jiang *et al.* reported current-induced switching (CIS) of a spin-valve system using a CoGd free layer and found that magnetoresistance and CIS showed different temperature dependence [39], with the former showing an anomaly near T_{M} and the latter near T_{A}. Our results do not indicate any obvious anomalies in either spin transport or SOTs other than near T_{M}. Finley and Liu also concluded that $\chi_{\mathrm{DL}} \propto \frac{1}{M_{\mathrm{s}}}$ based on a composition-dependence study in TbCo [32], and suggested that past studies on ultrafast switching and CIS using conventional spin-transfer torque may involve different physical mechanisms than the case of SOTs. The reasons why the current-induced effective fields track

the net magnetization rather than the net angular momentum remains to be understood. Finally, we note that while this paper was under review, a study of temperature-dependent spin-orbit torques in Pt/GdCoFe was reported [49], which found an enhanced dampinglike torque near T_M, consistent with our results.

In conclusion, we have examined the temperature dependence of magnetic properties and spin transport in bilayer $Ta/Tb_{19}Co_{81}$ films with bulk PMA. Magnetic properties vary as a function of temperature, indicating that they are dominated by the net magnetization. Despite the clear sign change of R_{AHE} as T crosses T_M, the magnitude of R_{AHE} remains almost constant, suggesting that it is related to spin-dependent interactions with the TM sublattice. By performing conventional harmonic voltage measurement, the temperature dependences of the SOT effective fields and the spin-torque efficiency were quantified. It was found that χ_{DL} is much larger than χ_{FL}, and χ_{DL} varies inversely with net magnetization, whereas χ_{FL} is relatively constant. By contrast, the spin-torque efficiency, which accounts for the varying M_s, shows no significant temperature dependence, and since the spin Hall angle of Ta is expected to likewise vary weakly with temperature in our experimental range, the results suggest that the spin-mixing conductance does not depend on the net magnetization of the ferrimagnet. Finally, we point out that although χ_{DL} tends to diverge near T_M, both $\mu_0 H_c$ and $\mu_0 H_{an}$ also diverge, which might mitigate advantages for SOT switching. Nonetheless, highly efficient SOTs in bulk-PMA magnetic thin films with highly tunable properties make these materials attractive for potential device applications.

We thank Dr. C. O. Avci and Professor Chi-Feng Pai for fruitful discussion. This work was supported by the National Science Foundation under NSF-ECCS-1408172 and by the Samsung SGMI program.

[1] M. Miron, K. Garello, G. Gaudin, P.-J. Zermatten, M. V. Costache, S. Auffret, S. Bandiera, B. Rodmacq, A. Schuhl, and P. Gambardella, Nature (London) **476**, 189 (2011).
[2] L. Liu, C.-F. Pai, Y. Li, H. W. Tseng, D. C. Ralph, and R. A. Buhrman, Science **336**, 555 (2012).
[3] I. M. Miron, G. Gaudin, S. Auffret, B. Rodmacq, A.Schuhl, S. Pizzini, J. Vogel, and P. Gambardella, Nat. Mater. **9**, 230 (2010).
[4] S. Emori, T. Nan, A. M. Belkessam, X. Wang, A. D. Matyushov, C. J. Babroski, Y. Gao, H. Lin, and N. X. Sun, Phys. Rev. B **93**, 180402 (2016).
[5] L. Liu, O. J. Lee, T. J. Gudmundsen, D. C. Ralph, and R. A. Buhrman, Phys. Rev. Lett. **109**, 096602 (2012).
[6] J. Kim, J. Sinha, M. Hayashi, M. Yamanouchi, S. Fukami, T. Suzuki, S. Mitani, and H. Ohno, Nat. Mater. **12**, 240 (2013).
[7] C.-F. Pai, L. Liu, Y. Li, H. W. Tseng, D. C. Ralph, and R. A. Buhrman, Appl. Phys. Lett. **101**, 122404 (2012).
[8] K. Garello, I. M. Miron, C. O. Avci, F. Freimuth, Y. Mokrousov, S. Blügel, S. Auffret, O. Boulle, G. Gaudin, and P. Gambardella, Nat. Nanotechnol. **8**, 587 (2013).
[9] C. O. Avci, K. Garello, C. Nistor, S. Godey, B. Ballesteros, A. Mugarza, A. Barla, M. Valvidares, E. Pellegrin, A. Ghosh, I. M. Miron, O. Boulle, S. Auffret, G. Gaudin, and P. Gambardella, Phys. Rev. B **89**, 214419 (2014).
[10] C. O. Avci, K. Garello, M. Gabureac, A. Ghosh, A. Fuhrer, S. F. Alvarado, and P. Gambardella, Phys. Rev. B **90**, 224427 (2014).
[11] C.-F. Pai, M. H. Nguyen, C. Belvin, L. H. Vilela-Leao, D. C. Ralph, and R. A. Buhrman, Appl. Phys. Lett. **104**, 082407 (2014).
[12] X. Qiu, P. Deorani, K. Narayanapillai, K.-S. Lee, K.-J. Lee, H.-W. Lee, and H. Yang, Sci. Rep. **4**, 4491 (2014).
[13] S. Woo, M. Mann, A.-J. Tan, L. Caretta, and G. S. D. Beach, Appl. Phys. Lett. **105**, 212404 (2014).
[14] T. Nan, S. Emori, C.-T. Boone, X. Wang, T.-M. Oxholm, J.-G. Jones, B.-M. Howe, G.-J. Brown, and N.-X. Sun, Phys. Rev. B **91**, 214416 (2015).
[15] Q. Hao and G. Xiao, Phys. Rev. B **91**, 224413 (2015).
[16] K.-F. Huang, D.-S. Wang, H.-H. Lin, and C.-H. Lai, Appl. Phys. Lett. **107**, 232407 (2015).
[17] C.-F. Pai, Y. Ou, L. H. Vilela-Leão, D. C. Ralph, and R. A. Buhrman, Phys. Rev. B **92**, 064426 (2015).
[18] C.-F. Pai, M. Mann, A. J. Tan, and G. S. D. Beach, Phys. Rev. B **93**, 144409 (2016).
[19] K. Ueda, C.-F. Pai, A. J. Tan, M. Mann, and G. S. D. Beach, Appl. Phys. Lett. **108**, 232405 (2016).
[20] M.-H. Nguyen, D. C. Ralph, and R. A. Buhrman, Phys. Rev. Lett. **116**, 126601 (2016).
[21] J. Yu, X. Qiu, W. Legrand, and H. Yang, Appl. Phys. Lett. **109**, 042403 (2016).
[22] M. Akyol, W. Jiang, G. Yu, Y. Fan, M. Gunes, A. Ekicibil, P. K. Amiri, and K. L. Wang, Appl. Phys. Lett. **109**, 022403 (2016).
[23] M.-H. Nguyen, M. Zhao, D. C. Ralph, and R. A. Buhrman, Appl. Phys. Lett. **108**, 242407 (2016).
[24] J. Yu, X. Qiu, Y. Wu, J. Yoon, P. Deorani, J. M. Besbas, A. Manchon, and H. Yang, Sci. Rep. **6**, 32629 (2016).
[25] Y. Ou, C.-F. Pai, S. Shi, D. C. Ralph, and R. A. Buhrman, Phys. Rev. B **94**, 140414(R) (2016).
[26] S. Emori, U. Bauer, S. M. Ahn, E. Martinez, and G. S. D. Beach, Nat. Mater. **12**, 611 (2013).
[27] K.-S. Ryu, L. Thomas, S.-H. Yang, and S. S. P. Parkin, Nat. Nanotechnol. **8**, 527 (2013).
[28] J. Torrejon, J. Kim, J. Sinha, S. Mitani, M. Hayashi, M. Yamanouchi, and H. Ohno, Nat. Commun. **5**, 4655 (2014).
[29] K. Ueda, K. J. Kim, Y. Yoshimura, R. Hiramatsu, T. Moriyama, D. Chiba, H. Tanigawa, T. Suzuki, E. Kariyada, and T. Ono, Appl. Phys. Express **7**, 053006 (2014).
[30] T. Taniguchi, K.-J. Kim, Y. Yoshimura, T. Moriyama, H. Tanigawa, T. Suzuki, E. Kariyada, and T. Ono, Appl. Phys. Express **7**, 053005 (2014).
[31] D. Bang, J. Yu, X. Qiu, Y. Wang, H. Awano, A. Manchon, and H. Yang, Phys. Rev. B **93**, 174424 (2016).
[32] J. Finley and L. Liu, Phys. Rev. Appl. **6**, 054001 (2016).
[33] K. Ueda, M. Mann, C.-F. Pai, A.-J. Tan, and G. S. D. Beach, Appl. Phys. Lett. **109**, 232403 (2016).

[34] P. Hansen, C. Clausen, G. Much, M. Rosenkranz, and K. J. Witter, Appl. Phys. **66**, 756 (1989).
[35] C. D. Stanciu, A. V. Kimel, F. Hansteen, A. Tsukamoto, A. Itoh, A. Kirilyuk, and Th. Rasing, Phys. Rev. B **73**, 220402(R) (2006).
[36] M. Binder, A. Weber, O. Mosendz, G. Woltersdorf, M. Izquierdo, I. Neudecker, J. R. Dahn, T. D. Hatchard, J.-U. Thiele, C. H. Back, and M. R. Scheinfein, Phys. Rev. B **74**, 134404 (2006).
[37] C. D. Stanciu, F. Hansteen, A. V. Kimel, A. Kirilyuk, A. Tsukamoto, A. Itoh, and Th. Rasing, Phys. Rev. Lett. **99**, 047601 (2007).
[38] S. Alebrand, M. Gottwald, M. Hehn, D. Steil, M. Cinchetti, D. Lacour, E. E. Fullerton, M. Aeschlimann, and S. Mangin, Appl. Phys. Lett. **101**, 162408 (2012).
[39] X. Jiang, L. Gao, J. Z. Sun, and S. S. P. Parkin, Phys. Rev. Lett. **97**, 217202 (2006).
[40] D.-T. Ngo, K. Ikeda, and H. Awano, Appl. Phys. Express **4**, 093002 (2011).
[41] D. Bang and H. Awano, Appl. Phys. Express **5**, 125201 (2012).
[42] T. Tono, T. Taniguchi, K.-J. Kim, T. Moriyama, A. Tsukamoto, and T. Ono, Appl. Phys. Express **8**, 073001 (2015).
[43] Z. Zhao, M. Jamali, A. K. Smith, and J.-P. Wang, Appl. Phys. Lett. **106**, 132404 (2015).
[44] N. Roschewsky, T. Matsumura, S. Cheema, F. Hellman, T. Kato, S. Iwata, and S. Salahuddin, Appl. Phys. Lett. **109**, 112403 (2016).
[45] T. Okuno, K-J. Kim, T. Tono, S. Kim, T. Moriyama, H. Yoshikawa, A. Tsukamoto, and T. Ono, Appl. Phys. Express **9**, 073001 (2016).
[46] J. Kim, P. Sheng, S. Takahashi, S. Mitani, and M. Hayashi, Phys. Rev. Lett. **116**, 097201 (2016).
[47] B. I. Min and Y.-R. Jang, J. Phys.: Condens. Matter **3**, 5131 (1991).
[48] J. M. D. Coey, *Rare-Earth Iron Permanent Magnets* (Clarendon, New York, 1996).
[49] W. S. Ham, S. Kim, D.-H. Kim, K.-J. Kim, T. Okuno, H. Yoshikawa, A. Tsukamoto, T. Moriyama, and T. Ono, Appl. Phys. Lett. **110**, 242405 (2017).